Available online at www.sciencedirect.com
ScienceDirect
Atmospheric Environment 41 (2007) 2061–2072
ATMOSPHERIC ENVIRONMENT
www.elsevier.com/locate/atmosenv

Atmospheric polycyclic aromatic hydrocarbons observed over the North Pacific Ocean and the Arctic area: Spatial distribution and source identification

Xiang Ding[a,c], Xin-Ming Wang[a,*], Zhou-Qing Xie[b], Cai-Hong Xiang[a,c], Bi-Xian Mai[a], Li-Guang Sun[b], Mei Zheng[d], Guo-Ying Sheng[a], Jia-Mo Fu[a], Ulrich Pöschl[e]

[a]*State Key Laboratory of Organic Geochemistry, Guangzhou Institute of Geochemistry, Chinese Academy of Sciences, Guangzhou 510640, China*
[b]*School of Earth and Space Sciences, University of Science and Technology of China, Hefei 230026, China*
[c]*Graduate School of Chinese Academy of Sciences, Guangzhou 510640, China*
[d]*School of Earth and Atmospheric Sciences, Georgia Institute of Technology, Atlanta, GA 30332, USA*
[e]*Biogeochemistry Department, Max-Plank Institute for Chemistry, D-55128 Mainz, Germany*

Received 7 August 2006; received in revised form 31 October 2006; accepted 1 November 2006

Abstract

During the 2003 Chinese Arctic Research Expedition from the Bohai Sea to the high Arctic (37–80°N) aboard the icebreaker Xuelong (Snow Dragon), air samples were collected using a modified high-volume sampler that pulls air through a quartz filter and a polyurethane foam plug (PUF). These filters and PUFs were analyzed for particulate phase and gas phase polycyclic aromatic hydrocarbons (PAHs), respectively, in the North Pacific Ocean and adjacent Arctic region. The $\sum$PAHs (where $\sum = 15$ compounds) ranged from undetectable level to 4380 pg m^{-3} in the particulate phase and 928–92 600 pg m^{-3} in the gas phase, respectively. A decreasing latitudinal trend was observed for gas-phase PAHs, probably resulting from temperature effects, dilution and decomposition processes; particulate-phase PAHs, however, showed poor latitudinal trends, because the effects of temperature, dilution and photochemistry played different roles in different regions from middle-latitude source areas to the high latitudes. The ratios of PAH isomer pairs, either conservative or sensitive to degradation during long-range transport, were employed to interpret sources and chemical aging of PAHs in ocean air. In this present study the fluoranthene/pyrene and indeno[123-cd]pyrene/benzo[ghi]pyrene isomer pairs, whose ratios are conservative to photo-degradation, implies that biomass or coal burning might be the major sources of PAHs observed over the North Pacific Ocean and the Arctic region in the summer. The isomer ratios of 1,7/(1,7 + 2,6)-DMP (dimethylphenanthrene) and anthracene/phenanthrene, which are sensitive to aging of air masses, not only imply chemical evolving of PAHs over the North Pacific Ocean were different from those over the Arctic, but reveal that PAHs over the Arctic were mainly related to coal burning, and biomass burning might have a larger contribution to the PAHs over the North pacific ocean.

Keywords: Polycyclic aromatic hydrocarbons (PAHs); Arctic; North Pacific Ocean; Biomass burning

*Corresponding author. Tel.: +86 20 85290180; fax: +86 20 85290706.
E-mail address: wangxm@gig.ac.cn (X.-M. Wang).

1352-2310/$ - see front matter © 2006 Elsevier Ltd. All rights reserved.
doi:10.1016/j.atmosenv.2006.11.002

1. Introduction

Polycyclic aromatic hydrocarbons (PAHs) are formed by incomplete combustion or pyrolysis of materials containing carbon and hydrogen. They have both anthropogenic and natural sources. The former includes combustion processes of fossil fuels and biomass burning, and the release of uncombusted petroleum products; the latter includes natural fires and diagenetic processes (Simoneit, 1984). As a group of semi-volatile organic compounds (SVOCs), PAHs are ubiquitous and detected in a variety of environmental media, including air (Halsall et al., 1994; Buehler et al., 2001), soil (Motelay-Massei et al., 2004), sediment (Laflamme and Hites 1978; Mai et al., 2003) and biological samples (Page et al., 2004). Due to their lipophilicity and hydrophobicity, PAHs may partition and accumulate in organisms and thus have carcinogenic and mutagenic activity (Okona-Mensah et al., 2005; Perera et al., 2005).

The occurrence and sources of PAHs in the atmosphere have been widely studied. In most urban and rural areas, airborne PAHs originate mainly from automobile exhausts and/or combustion of fossil fuel (Mai et al., 2003; Ohura et al., 2004), while in remote areas, such as in open ocean air and the Arctic, both biomass burning and fossil fuel combustion may contribute to PAHs. Crimmins et al. (2004) analyzed particulate PAHs, organic carbon (OC), elemental carbon (EC), SO_4^{2-}, and K^+ in the atmosphere of Atlantic and Indian Ocean. They pointed out that fossil fuel combustion, rather than biomass burning, was the predominant source of PAHs in the Northern Hemisphere Indian Ocean atmosphere. However, few studies have been conducted in the North Pacific Ocean and the adjacent Arctic Ocean. In the Arctic, Daisey et al. (1981) measured particulate organic matter (POM), PAHs, and ^{210}Pb in the Arctic aerosol in Barrow, Alaska. They found that the principal source of PAHs was fossil fuel combustion in the mid-latitude regions in winter from the presence of fly ash and seasonal changes in organic species, ^{210}Pb and meteorology.

Seasonal changes in meteorology are key factors in determining the chemical composition of the Arctic atmosphere. In winter, the pollutants in Eurasia and North America can move into the Arctic region easily and rapidly by atmospheric transportation. In the Arctic haze, air mass back trajectories (BTs) analysis for February 1994 revealed long-range transport from Eurasia into the high Arctic (Halsall et al., 1997). In summer the meteorological barrier, however, will make the influence of northward transport from low latitudes weaker. Thus the variety of meteorology may lead to the seasonal change of sources of PAHs in the Arctic atmosphere. Slater et al. (2002) reported PAHs and radiocarbon (^{14}C) of EC in water-insoluble particles from a snow pit excavated at Summit, Greenland in 1996. They used the ratios of BghiP/BeP and Ret/BeP to quantify the relative contribution of fossil fuel and biomass combustion, and ^{14}C measurements to distinguish EC between the two sources. Results showed that fossil fuel combustion was dominant in spring, and biomass burning impacted deeply in fall to early winter, while both sources had influences in summer.

In July to September 2003, ship-board air samples were collected along a cruise from Bohai Sea to the North Pole Area (37–80°N). Detailed information about this expedition has been described elsewhere (Wang et al., 2005). In the present study, the purposes are to determine the spatial distribution of PAHs from mid-latitude source areas to the high Arctic, and to provide information about the long-range atmospheric transport (LRAT) and possible sources of PAHs in the North Pacific Ocean and adjacent Arctic Ocean during warm periods.

2. Experimental section

2.1. Field sampling

A total of 49 particle samples, 30 of which had vapor samples collected simultaneously, were taken aboard the expedition cruise from Bohai Sea (37.78°N, 123.12°E) to the Arctic (80.22°N, 146.75°W) between 11 July–21 September 2003. The sampling route is shown in Fig. 1. A modified high volume air sampler was placed windward on the uppermost front deck of the ship for simultaneous sampling of PAHs in particulate and gas phases. Air was drawn at a flow rate of $\sim 1.0\,m^3\,min^{-1}$ through a quartz fiber filter (QFF) (Whatman QM-A, 20.3×25.4 cm) to collect total suspended particles (TSP) from the air stream, followed by one-and-a-half polyurethane foam plug (PUF, 6.5 cm diameter $\times$ 8 cm height) contained in an aluminum cylinder to trap the gas-phase compounds. The sampled air volumes ranged from 1215 to $3030\,m^3$ (at 0 °C and 1 atm). The back half PUF served as an indicator of breakthrough of

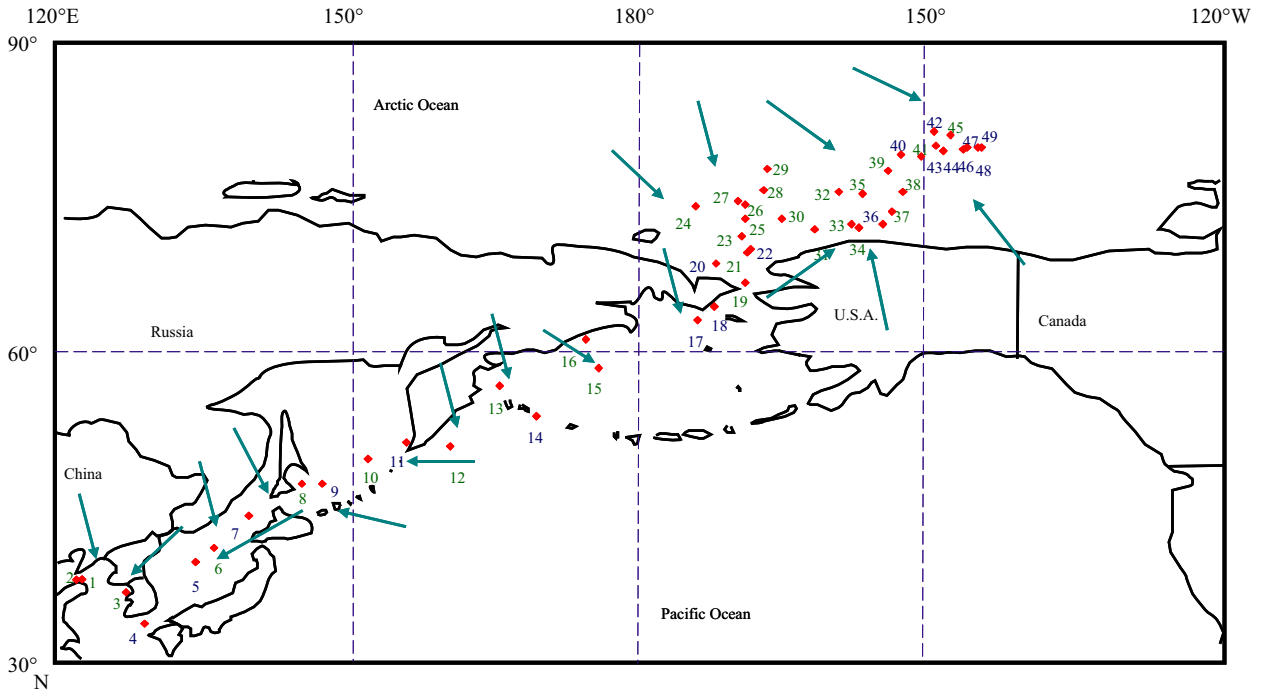

Fig. 1. The sample route of CHINARE 2003 and broad origins of the air means. Green means both QFF and PUF samples are collected (sites 1–3,6,8,10,12,13,15,16,19,21,23–35,37–39,41,45), blue means only QFF samples are collected (other sites) (for interpretation of the references to color in this figure legend, the reader is referred to the web version of this article).

gas-phase. In order to remove possible organic impurities, before field use, the QFFs were heated at 450 °C for 4 h, and the PUFs were Soxhlet extracted for 24 h with methanol and dichloromethane (DCM). Then the QFFs and PUFs were wrapped in aluminum foil and zipped in Teflon bags. After sampling, the filters and PUFs were again wrapped in aluminum foil and zipped in Teflon bags, and stored in freezers at −20 °C until analysis. In addition, three clean QFFs and PUFs were exposed to the atmosphere during the sampling period and processed as field blanks.

2.2. Sample extraction

A detailed description of the analytical procedure for PAHs has been published elsewhere (Bi et al., 2003). Briefly, prior to 72 h Soxhlet extraction with redistilled DCM, a mixture of deuterated PAH standards (acenaphthene-d10, phenantgrene-d10, chrysene-d12, and perylene-d12) was added to all samples as surrogate compounds. The extracts were concentrated and solvent-exchanged to redistilled hexane, and then purified using a 1:2 alumina/silica column chromatography. The first fraction, containing aliphatic hydrocarbons, was eluted with 30 mL of hexane. The second fraction, containing PAHs, was collected by eluting 70 mL of DCM/hexane (3:7 v/v). The latter was then concentrated to a final volume of 200 μL under a gentle stream of nitrogen. Eight microliters of 50 μg mL^{-1} hexamethylbenzene (Aldrich Chemicals, Gillingham, Dorset, USA), was added to the samples as an internal standard before instrumental analysis.

2.3. Instrumental analysis and parameters

PAHs were analyzed by an Agilent 6890N gas chromatograph (GC) coupled to an Agilent 5973N mass selective detector in the selective ion monitoring mode. The GC column used was a 50 m HP-5 capillary column (0.32 mm i.d., 0.17 μm film thickness). The column temperature was initiated at 80 °C (held for 2 min) and increased to 290 °C at 4 °C min^{-1} (held for 30 min). Data for the 20 PAHs quantified in this study are listed in Table 1. The method detection limit (MDL), defined as three times the noise level, ranged from 0.6 pg m^{-3} for acenaphthylene to 7.0 pg m^{-3} for coronene, when calculated with the average sampling volume of

Table 1
Summary of measured PAHs ranges (pg m^{-3})

	Diagnostic MDL ion (m/z)		Far East Asia (sites 1–9)						North Pacific Ocean (sites 10–19)						Arctic (sites 20–49)					
			16.3 (8.7–21.5)[a]						8.5 (3.6−10.6)						−1.2 (−3.4–5.8)					
			Particulate			Gas			Particulate			Gas			Particulate			Gas		
			($n = 9$)			($n = 5$)			($n = 10$)			($n = 6$)			($n = 29$)			($n = 18$)		
			Geometric mean[b]	Arithmetic mean[b]	Range[d]	Geometric mean	Arithmetic mean	Range	Geometric mean	Arithmetic mean	Range	Geometric mean	Arithmetic mean	Range	Geometric mean	Arithmetic mean	Range	Geometric mean	Arithmetic mean	Range
Acenaphthylene (Acl)	152	0.6	1.5	2.8	0.3–7.4	136	199	54.7–557	0.3	0.3	0.3–0.8	61.3	64.6	34.0–102	0.9	1.4	0.3–5.8	47.4	53.5	16.5–111
Acenaphthene (Ace)	154	0.6	1.7	4.2	0.3–13.1	224	363	86.9–1060	0.6	0.9	0.3–3.3	86.5	97.3	43.6–198	2.5	5.1	0.3–22.2	59.3	91.0	6.1–409
Fluorine (Fl)	166	1.4	4.3	8.7	0.7–34.1	2670	3650	1220–8770	1.1	1.3	0.7–3.5	1380	1510	724–2450	3.4	9.6	0.7–50.9	644	742	183–1440
Phenanthrene (Phe)	178	1.5	37.2	72.8	9.2–261	18 500	26 600	4850–53 500	4.4	9.5	0.8–28.1	6700	7350	3610–12 100	8.7	56.6	0.8–500	1610	1820	477–3560
Anthracene (An)	178	2.1	2.7	8.7	1.1–36.7	3190	4680	806–9350	1.2	1.3	1.1–3.4	990	1080	529–1860	1.9	3.7	1.1–22.1	226	262	59.6–607
2,6-dimethylphenanthrene (2,6–DMP)[c]	206	1.5	1.3	2.6	0.8–12.7	64.8	162	11.0–391	1.3	3.9	0.8–30.3	37.6	72.6	17.8–299	2.3	8.6	0.8–91.1	20.5	28.7	4.8–76.1
1,7-dimethylphenanthrene (1,7-DMP)[c]	206	1.5	2.9	5.8	0.8–22.0	209	431	33.3–1110	1.6	4.2	0.8–29.9	64.1	81.6	39.2–238	2.6	11.2	0.8–125	24.2	29.1	8.3–70.3
Fluoranthene (Flu)	202	2.0	35.0	126	1.0–456	3630	7130	522–17 300	6.0	11.0	1.0–43.9	682	740	344–1150	11.9	82.2	1.0–810	176	198	80.1–424
Pyrene (Py)	202	1.9	25.8	106	0.9–404	1960	4000	280–9940	2.4	6.3	0.9–28.5	373	401	192–603	9.4	49.5	0.9–381	117	133	57.4–296
Retene (Ret)[c]	234	1.5	7.8	10.7	0.8–20.8	151	324	22.0–829	5.4	6.0	0.8–11.9	26.1	27.5	15.7–39.6	2.6	4.9	0.8–25.9	5.9	6.9	1.2–14.6
Benzo[a]anthracene (BaA)	228	5.6	16.2	78.9	2.8–322	11.9	33.8	2.8–138	4.8	11.9	2.8–71.0	5.2	8.1	2.8–23.9	9.2	25.5	2.8–164			
Chrysene (Chr)	228	5.6	35.5	136	2.8–506	39.2	78.8	9.2–272	11.0	39.6	2.8–169	13.8	20.6	2.8–60.0	22.4	69.8	2.8–374	5.3	6.3	2.8–13.2
Benzo[b]fluoranthene (BbF)	252	4.7	29.7	144	2.4–569				5.5	14.7	2.4–67.4				14.0	48.2	2.4–391			
Benzo[k]fluoranthene (BkF)	252	3.7	11.8	63.5	1.8–254				2.5	3.9	1.8–20.6				5.5	18.0	1.8–136			
Benzo[e]pyrene (BeP)[c]	252	5.5	48.6	228	2.8–907				11.5	34.7	2.8–190				22.6	62.4	2.8–319			
Benzo[a]pyrene (BaP)	252	5.5	24.2	147	2.8–612				3.9	10.7	2.8–82.3				4.6	10.4	2.8–127			
Indeno[123-cd]pyrene (InP)	276	4.6	29.7	187	2.3–773				4.4	12.0	2.3–84.3				15.5	57.1	2.3–410			
Dibenzo[a,h]anthracene (DBahA)	278	3.7	5.4	16.5	1.8–71.0				2.4	3.1	1.8–12.8				2.2	2.8	1.8–14.0			
Benzo[ghi]pyrene (BghiP)	276	3.1	16.6	101	1.5–416				2.6	8.4	1.5–66.1				10.5	36.4	1.5–222			
Coronene (Cor)[c]	300	7.0	8.4	26.4	3.5–107				3.9	4.3	3.5–11.6				6.6	14.7	3.5–131			
∑PAH[c]		46.6	319	1200	32.7–4380	31300	46 700	8160–92 600	68.7	135	24.7–632	10 400	11 300	6130–18 000	169	476	23.3–2640	2940	3310	928–6310

[a]Mean temperature (°C) with range of temperature in brackets.
[b]Half of MDL was assigned to values <MDLs when computing mean and sum.
[c]Not included in the ∑ concentration.
[d]Half of MDL is used if the minimum level is less than MDL.

2051 m^3. Half of MDL was assigned to values <MDL when computing mean and sum.

2.4. Quality control/quality assurance

Three field blanks and six laboratory blanks (solvent with a QFF and PUF identical to that used to collect the air samples) were processed. Laboratory and field blanks were extracted and analyzed in the same way as field samples. There was no difference between concentrations of analytes in the laboratory and field blanks, indicating that contamination was negligible during sampling, transport, and storage. Only very low concentrations of Phe were detected in the PUFs of field blanks, and they were subtracted from those in the sample extracts. Surrogate recoveries ($n = 97$, both field and laboratory control samples) were $87 \pm 15\%$ for acenaphthene-d10, $98 \pm 15\%$ for phenanthrene-d10, $90 \pm 16\%$ for chrysene-d12, and $84 \pm 16\%$ for perylene-d12, respectively. The relative differences for individual PAHs in paired duplicate samples ($n = 3$) were all <15%. Recoveries of PAHs in spiked blank samples (PAH standards spiked into solvent with clean QFFs and PUFs, $n = 6$), matrix spiked samples (PAH standards spiked into pre-extracted QFFs and PUFs, $n = 6$), and National Institute of Standards and Technology (NIST; Gaithersburg, MD) 1941 reference samples ($n = 3$) ranged from 77% to 104%, 72% to 98%, and 80% to 120%, respectively. The reported results were not adjusted using recovery rate. Sampling breakthrough is not a problem at this study, with only a few of the lighter PAHs detected in the backup PUF (<20% of the total gas phase compound).

2.5. General remarks on the contamination of shipboard air samples

There is always a potential for possible contamination of ship-based air samples. Emissions from the ship and/or from the ship's funnel would be particularly important for combustion-derived pollutants such as PAHs, and polychlorinated dibenzo-*p*-dioxins and dibenzofurans (Lohmann et al., 2004). In this study, samples were collected upwind in the uppermost front deck to avoid such contamination. As discussed later in detail, both the low ratios of more reactive to less reactive PAHs and the ratios of PAH isomer pairs indicated that the air masses were relatively aged, and that contamination from ship emissions was avoided well for the air samples collected. Cooper (2001) reported exhaust emissions from different ships. Two-ring PAHs were found to be the dominant compounds and concentrations of the heavy PAHs (molecular weight >228) were below the detection limits in most samples. The composition patterns of PAHs from our measurements were quite different from those of typical emissions from ships. The significant difference between air sample 26 (Fig. 1) and other samples also provided evidence that samples were not contaminated by ship emissions. During the collection of sample 26, the ship had stopped at the Port of Barrow in north Alaska to pick up some foreign scientists. Therefore this sample might be affected by the ship emissions, as can be seen from its much higher BaP/BeP ratio (1.1) compared to those (<0.7) in all other samples (Khalili et al., 1995). Sample 26 was therefore excluded from the discussion below, except in Fig. 3.

2.6. Back trajectories

Air mass origins were determined for the cruise samples using the HYSPLIT transport and dispersion model from the NOAA Air Resources Laboratory (Draxler and Rolph, 2003). Two BTs were performed, for the start and end of each sampling episode. BTs were traced for 5 days with 6 h steps at 100, 500 and 1000 m above sea level. Fig. 1 shows a general indication of the direction of the air mass origins. It should be noted that some uncertainties are associated with the BTs as the ship was changing location (Stohl et al., 2002).

3. Results and discussion

3.1. Air concentrations and spatial distribution

Table 1 presents the concentrations of 20 PAHs. The sum of the 16 USEPA priority PAHs is often used to make comparisons among different studies. Naphthalene is in the list of the 16 USEPA priority PAHs, but due to its high volatility and low recovery for particulate samples, its levels were not quantified in the present study, so we only presented the sum of 15 PAHs ($\sum$PAHs) with naphthalene being excluded, as did in many previous studies.The $\sum$PAHs ranged from undetectable level to 4380 pg m^{-3} for the particulate phase and 928–92600 pg m^{-3} for the gas phase, respectively.

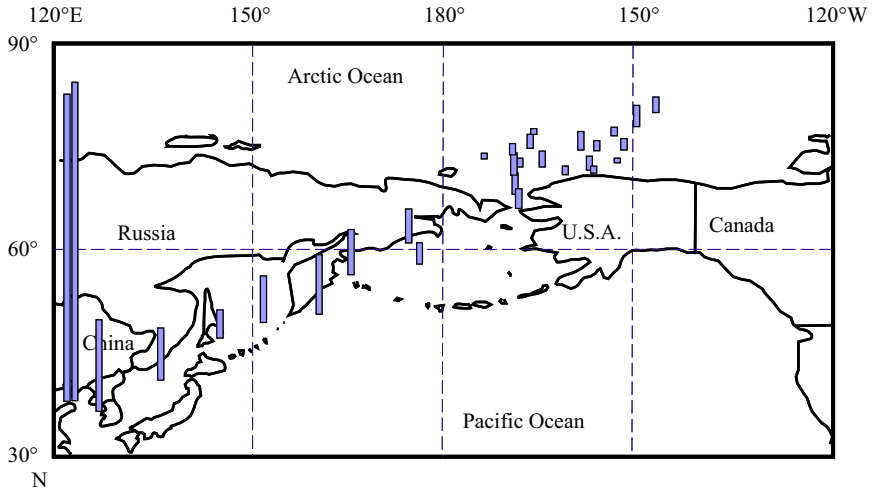

Fig. 2. Spatial distribution of ∑PAHs (particle + gas) along the cruise ($n = 29$). Concentrations are displayed at the average sampling locations (bars), with highest bar representing 97 000 pg m^{-3} (site 1).

The levels of particulate phase PAHs were similar to the Atlantic Ocean and Northern Indian Ocean atmosphere (Crimmins et al., 2004) in January to March. The levels of gas phase PAHs were higher than those reported in the Atlantic Ocean atmosphere in January to March (Jaward et al., 2004). Phenanthrene was the dominant compound among the gas phase PAHs, contributing ~50% to ∑PAHs. The 2–4 rings PAHs, from Acl to Py, occurred dominantly in the gas phase; and heavy PAHs, from BbF to Cor, existed only in the aerosol fraction. The highest concentration, above 90 000 pg m^{-3}, occurred near the Liaodong peninsula (sites 1 and 2, Fig. 1).

Fig. 2 shows the spatial distribution of ∑PAHs (gas + particulate) along the cruise. Higher levels occurred in Far East Asia (34–48°N, 122–148°E) including the Bohai Sea and the Japan Sea, with an arithmetic mean of 48 500 pg m^{-3}, which was lower than those of some adjacent continental areas, such as Qingdao (87.5 ng m^{-3}) (Guo et al., 2003), Seoul (89.3 ng m^{-3}) (Park et al., 2002), Fuji (365 ng m^{-3}) and Shimizu (270 ng m^{-3}) (Ohura et al., 2004). In the higher latitudinal regions of the North Pacific Ocean (48–66°N), a lower mean total concentration of 11400 pg m^{-3} was obtained. In the Arctic (>66.7°N), the mean concentration was only 3530 pg m^{-3}, which was, however, higher than those reported in Dunnai, Alert and Tagish in May to September (Halsall et al., 1997), indicating the contamination of the Arctic area in summertime during our expedition.

3.2. Atmospheric processing

An, BaA and BaP are expected to be degraded more easily than their isomers during transportation due to their higher reactivity (Butler and Crossley, 1981). Using the ratios of a more reactive PAH to a less reactive PAH, such as An/Phe, BaA/Chr and BaP/Bep, a higher ratio indicates relatively little photochemical processing of the air mass and major impact from local emissions. On the other hand, a lower ratio is reflective of more aged PAHs. Therefore, it can be used to illustrate whether the air masses collected were fresh or aged. The degradation of gas phase PAHs is different from that of particulate phase PAHs. Gas phase PAHs are susceptible to degradation via OH radical; while particulate phase PAHs are susceptible to photo-degradation. The ratios of BaA/Chry were plotted against BaP/BeP for the samples collected during the cruise (Fig. 3). Because these four PAHs were not detected in most gaseous samples, only the particulate phase was considered. Generally, relatively higher ratios occurred in low latitude areas, and lower ratios existed in high latitude Arctic, showing that photo-degradation might be an important process during LRAT, especially for the particulate phase PAHs. The ratios of BaA/Chry and BaP/BeP in the particulate were significantly correlated with each other ($R^2 = 0.25$, $p < 0.05$, $n = 25$), suggesting that the two isomer pairs might share a similar transport pathway. BaP/BeP ≥ 1.0 had been reported for typical temperate urban

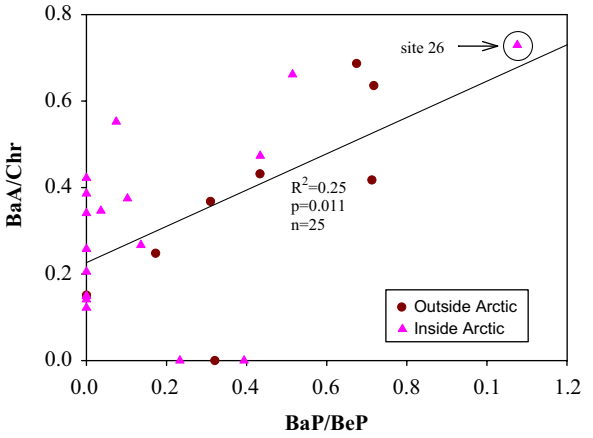

Fig. 3. Ratios of reactive/stable PAHs (BaP/BeP and BaA/Chr) in particulate phase in different regions during the expedition.

sources (Khalili et al., 1995). As shown in Fig. 3, most of the ratios were much lower than 1.0, indicating that the air masses were relatively aged. At sites 1, 2 and 5 near continental source areas in Far East Asia, the ratios of BaA/Chry and BaP/BeP were close to 0.7 and higher than other sites, suggesting air masses sampled at these sites were relatively fresh from the adjacent continental source areas. An and Phe predominantly occurred in the gas phase, and thus the ratio of An/Phe was more suitable to illustrate the degradation of gas phase PAHs.

The LRAT potential of SVOCs in air depends on temperature, compound reactivity and net depositional behavior (Wania et al., 1998; Wania, 2003). Dilution, deposition and decomposition processes and temperature effects will all impact on the air concentration during transportation (Goldan et al. 2000). In our study, gas phase $\sum$PAHs were significantly decreased with the increasing latitude ($r=-0.717$, $p<0.01$, $n=29$), while particulate phase $\sum$PAHs showed poor correlation with the latitude ($p>0.05$, $n=48$). In general, lower temperatures favor condensation of gas phase PAHs onto particulates. In this study, the relationships between $\sum$PAHs and the ratios of reactive to stable PAHs were also employed to elucidate the role of degradation in both phases during LRAT. Results revealed that $\sum$PAHs in the gas phase showed significant temperature dependence ($p<0.01$, $n=27$), and that gas phase $\sum$PAHs correlated well with the ratio of An/Phe ($r=0.41$, $p<0.05$, $n=27$). Particulate phase $\sum$PAHs correlated well with the ratios of BaA/Chry ($r=0.72$, $p<0.01$, $n=45$) and BaP/BeP ($r=0.31$, $p<0.05$, $n=45$). These good correlations all proved the important influence of degradation on the levels of PAHs in both gas and particulate phases. From middle latitudes to the high latitudes during the cruise, dilution, temperature effects and degradation processes (especially decomposition by the hytroxyl radical) would lead to the decrease of PAH levels in the gas phase. That is why decreasing trends with latitude in the gas phase were observed. It is interesting to see that the particulate-phase PAH over the North Pacific Ocean was lower than that in Arctic area. The highest particulate-phase PAH found in Fast East Asia was due to the vicinity of emission sources. The lowest level observed over the North Pacific Ocean was related to dilution and photo-degradation and, to lesser extent, the temperature effect. The medium level in Arctic area was likely caused by temperature effect which favored the condensation of gas-phase PAHs onto the particles. Under minus degree of temperature, it is unlikely that photo-degradation would be the significant atmospheric process though dilution could lower the particulate-phase PAHs level.

3.3. Source identification

As anthropogenic geochemical tracers, PAHs can be used to identify air masses from different source areas (Simoneit, 1984). The ratios of the principal parent PAHs with mass 178 (Phe and An), 202 (Flu and Py), 228 (BaA and Chry) and 276 (InP and BghiP) have been widely used to distinguish different sources in urban and rural areas (Bi et al., 2003; Cotham and Bidleman, 1995; Lohmann et al., 2000). But care should be taken when using these markers since the atmospheric degradation of BaP, BaA and An are much faster than their isomers or other parent PAHs (Kamens et al., 1988; Schauer et al., 1996). That is, the ratios of Phe/An, BaA/Chry and BaP/BeP will change with the aging of the air mass. The Flu/Py and InP/BghiP isomer pairs, however, photolytically degrade at comparable rates (Behymer and Hites, 1988; Masclet et al., 1986). Thus their ratios preserve the original compositional information during atmospheric transport, and might be applicable molecular markers for source evaluation in remote areas, such as ocean air. Yunker et al. (2002) summarized the results of different sources and proposed that for Flu/(Py+Flu) the petroleum boundary ratio appears close to 0.40, and the ratio between 0.40 and

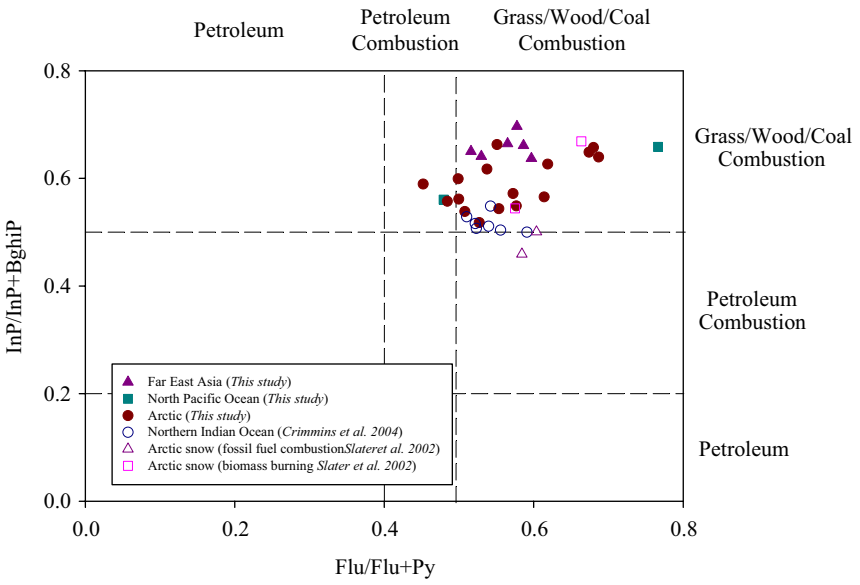

Fig. 4. Ratios of InP/BghiP + InP vs. Flu/Py + Flu in particulate phase in different regions.

0.50 is characteristic of petroleum combustion (liquid fossil fuel combustion), whereas a ratio >0.50 is characteristic of grass, wood or coal combustion; for InP/(BghiP + InP), a ratio <0.20 probably implies unburned petroleum (petrogenic source), 0.20–0.50 implies petroleum combustion (liquid fossil fuel combustion), and >0.50 implies grass, wood or coal combustion. Fig. 4 shows that the ratios of Flu/(Py + Flu) and InP/(BghiP + InP) in the particulate phase ranged from 0.45 to 0.77 and from 0.52 to 0.70, respectively. In the gas phase, the ratio of Flu/(Py + Flu) ranged from 0.53 to 0.67. All these ratios suggest that the combustion of biomass or coal might be the main sources of atmospheric PAHs in the North Pacific Ocean and the Arctic Ocean during the cruise.

To validate source markers employed in this study, data from other studies were also compared and plotted in Fig. 4. In the Northern Indian Ocean atmosphere, the ratios of Flu/(Py + Flu) and InP/(BghiP + InP) in the particulate were ranged from 0.51 to 0.59 and 0.47 to 0.55, respectively, and much closer to the boundaries (Fig. 4). This was consistent with the conclusion made by Crimmins et al. (2004) that a mixed combustion of biomass and fossil fuel influenced the ocean air, based on the significant correlations between selected PAHs and OC, EC, SO_4^{2-} and K^+. At Summit, Greenland, the typical snow samples predominantly impacted by fossil fuel combustion or biomass burning could be distinguished by measuring the radiocarbon (^{14}C) of EC and calculating the ratios of BghiP/BeP and Ret/BeP, as well as the changes in concentration of certain inorganic compounds (Slater et al., 2002). When the ratios of Flu/(Py + Flu) and InP/(BghiP + InP) were calculated for these snow samples typically representing different sources, the samples impacted by biomass burning were plotted in the area representing the combustion of grass, wood or coal; and the samples impacted by fossil fuel combustion were plotted in the area representing the same source (Fig. 4). Also the ratios of BghiP/BeP and Ret/BeP used by Slater et al. (2002) were calculated for the samples in this present study. Within the Arctic, the ratios of BghiP/BeP and Ret/BeP averaged 0.50 ± 0.28 and 0.08 ± 0.09, respectively. The much higher value of the former (representative of fossil fuel combustion) than that of the latter (representative of biomass burning) suggests that fossil fuel combustion, especially coal burning as indicated in Fig. 4, might be more important in the Arctic. In the area outside the Arctic, the two ratios averaged 0.22 ± 0.20 and 0.25 ± 0.30, respectively. This indicates that the two ratios did not point clearly to a particular source for samples outside the Arctic.

To distinguish between biomass burning and coal burning in the current study, the characteristics of two dimethylphenanthrene (DMP) isomers were also analyzed. The ratio of 1,7-DMP to 2,6-DMP

in air is a sensitive source indicator for distinguishing wood combustion from motor vehicle emissions. The ratio of 1,7-DMP/(1,7-DMP + 2,6-DMP) (abbreviated as 1,7/(1,7 + 2,6)-DMP) between 0.70 and 0.90 indicates wood combustion (Benner et al., 1995), while a ratio less than 0.42 indicates vehicle emissions (Benner et al., 1989). In brown coal combustion products, the ratio is ~0.62 (Grimmer et al., 1983). Other studies also found that the ratio of coal combustion is likely to be between that of wood combustion and vehicle emissions (Yunker et al., 2002). But the ratio of 1,7/(1,7 + 2,6)-DMP would decrease during LRAT since 1,7-DMP is unstable relative to 2,6-DMP. During our expedition, though the air masses were aged from BaP/BeP as discussed above, the ratio of 1,7/(1,7 + 2,6)-DMP still ranged from 0.44 to 0.82, above those typical for vehicle emissions and within those for biomass or coal burning.

Fig. 5 is the plot of 1,7/(1,7 + 2,6-DMP) against An/Phe in the gas phase. The ratio of the latter isomer pair also decreases during LRAT due to the faster degradation of An than Phe. Because these four compounds were dominant in the gas phase (>95% of the total of both phases), only gas phase data were used here. Available data show that emissions from coal burning (Chen et al., 2005; Oros and Simoneit, 2000) and biomass burning (Conde et al., 2005) had similar original ratio of An/Phe (~0.20). As shown in Fig. 5, the two isomer pair ratios were correlated well with each other both inside and outside the Arctic. In Far East Asia, the average ratio of 1,7/(1,7 + 2,6)-DMP was 0.76 ± 0.06, indicating biomass combustion to be the main source in this area. Although the same ratios ranged from 0.45 to 0.77 in the North Pacific Ocean, the good correlation between the two isomer pair ratios might imply that it was the aging during transportation that made the variation of 1,7/(1,7 + 2,6)-DMP. And biomass burning might also be the dominant source of atmospheric PAHs in the North Pacific Ocean during our study, since 1,7/(1,7 + 2,6)-DMP as high as 0.77 was not observed for coal burning. To identify the source areas out of the Arctic, the satellite data (results from the Along Track Scanning Radiometer (ATSR) on ESA's ERS-2 satellite) are used to see where biomass burning events had happened during sampling periods. During our cruise in North Pacific Ocean (11–31 July, 2003), ASTR active fire spots were shown in Fig. 6, and apparently there were great forest fires surrounding Russia's Lake

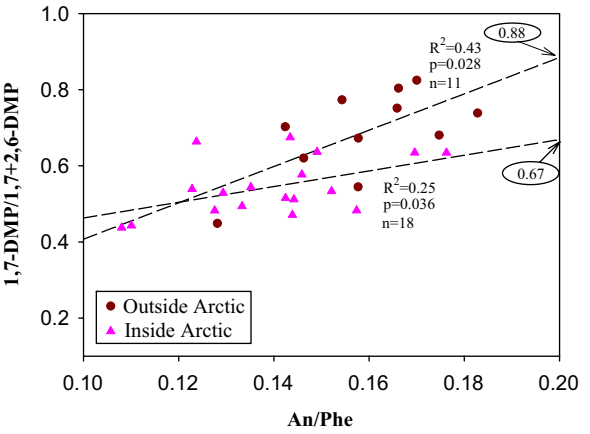

Fig. 5. PAH isomer ratios of 1,7/(1,7 + 2,6)-DMP vs. An/Phe in gas phase in different regions.

Baikal and east-coast areas (Fig. 6). Smoke from these fires had been streaming across eastern Russia and China and out over the Pacific Ocean off and on for months, and had traveled around the world, reaching Canada and the United States. Therefore the fires surrounding Russia's Lake Baikal and east-coast areas made a larger contribution to PAHs observed in the atmosphere of North Pacific Ocean during our expedition.

A flatter slope of 1,7/(1,7 + 2,6)-DMP against An/Phe in Fig. 5 was observed in the Arctic. The ratios of 1,7/(1,7 + 2,6)-DMP were between 0.44 and 0.67 with a mean value of 0.54 ± 0.08, implying aged air masses with biomass burning, or less aged air masses with coal burning, probably responsible for PAHs in the Arctic atmosphere in summer. Furthermore, if we consider biomass burning and coal burning both with a starting An/Phe of ~0.2, taking the dashed lines in Fig. 5 as "evolution" pathways, we would infer a starting 1,7/(1,7 + 2,6)-DMP of 0.88 and 0.67 for the North Pacific samples and the Arctic samples, respectively. This would suggest that the Arctic atmospheric PAHs during the study might be mainly related to coal burning. Simcik et al. (1999) measured the PAHs in the urban and adjacent coastal atmosphere of Chicago and Lake Michigan in 1994–1995, and suggested coal burning was the main source in both the urban and coastal air using a modified factor analysis-multiple regression model. They also reported the ratio of Flu/(Flu + Py) with a similar range (0.54–0.69) compared to the Arctic samples. It must be stressed that the original value of 0.2 for An/Phe should be

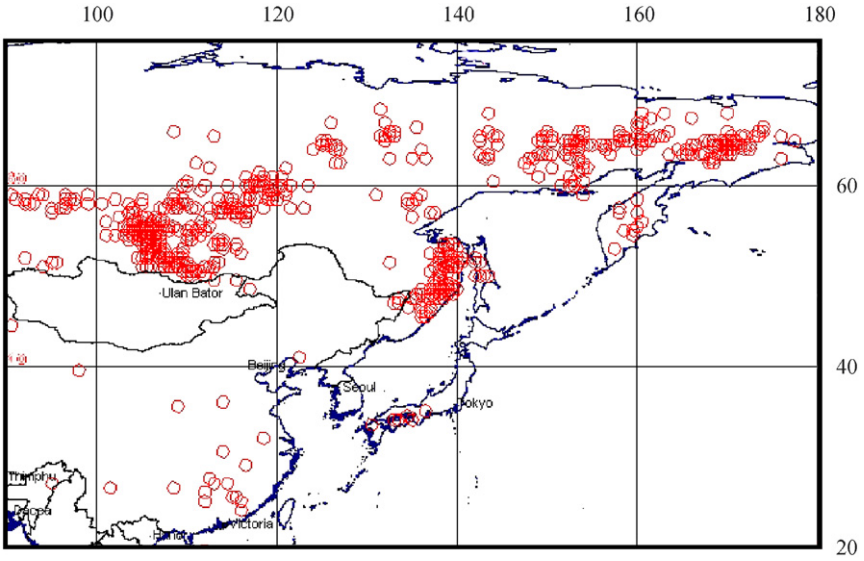

Fig. 6. Fire spots surrounding Russia's Lake Baikal and east-coast areas during our cruise in North Pacific Ocean recorded by the Along Track Scanning Radiometer (ATSR) on ESA's ERS-2 satellite. Red circles are fire spots (for interpretation of the references to color in this figure legend, the reader is referred to the web version of this article).

carefully used since the ratios may vary with different kinds of coal. Also we cannot make further comparisons with other researches due to too few data of two DMP isomers being available in field samples. Nevertheless, the present approach using two pairs of reactive isomers may provide a way to study the chemical evolution of air masses and identify the sources of atmospheric PAHs, especially when air masses are aged after LRAT, as from lower latitude source areas to the Arctic region.

Acknowledgments

The authors thank the financial support from Ministry of Science and Technology of China (2002CB410803 and 2003CB415002), the National Science Foundation of China (40673074), Ministry of Education of China (200354) and Chinese Academy of Sciences (KZCX3-SW-121). Without the technical assistance and convenience offered by the Chinese Antarctic and Arctic Administration and the crew of *Xuelong*, it would have been impossible for us to conduct the present study. The National Oceanic and Atmospheric Administration's Air Resources Laboratory is also gratefully acknowledged for the provision of the HYSPLIT transport and dispersion model and the READY website (http://www.arl.noaa.gov/ready.html) used in this study.

References

Behymer, T.D., Hites, R.A., 1988. Photolysis of polycyclic aromatic hydrocarbons adsorbed on fly ash. Environmental Science and Technology 22, 1311–1319.

Benner, B.A., Gordon, J.G.E., Wise, S.A., 1989. Mobile sources of atmospheric polycyclic aromatic hydrocarbons: a roadway tunnel study. Environmental Science and Technology 23, 1269–1278.

Benner, B.A., Wise, S.A., Currie, L.A., Klouda, G.A., Kline dinst, D.B., Zweidinger, R.B., Stevens, R.K., Lewis, C.W., 1995. Distinguishing the contributions of residential wood combustion and mobile source emissions using relative concentrations of dimethylphenanthrene isomers. Environmental Science and Technology 29, 2382–2389.

Bi, X., Sheng, G., Peng, P.a., Chen, Y., Zhang, Z., Fu, J., 2003. Distribution of particulate- and vapor-phase *n*-alkanes and polycyclic aromatic hydrocarbons in urban atmosphere of Guangzhou, China. Atmospheric Environment 37, 289–298.

Buehler, S.S., Basu, I., Hites, R.A., 2001. A comparison of PAH, PCB, and pesticide concentrations in air at two rural sites on Lake Superior. Environmental Science and Technology 35, 2417–2422.

Butler, J.D., Crossley, P., 1981. Reactivity of polycyclic aromatic hydrocarbons adsorbed on soot particles. Atmospheric Environment 15, 91–94.

Chen, Y., Sheng, G., Bi, X., Feng, Y., Mai, B., Fu, J., 2005. Emission factors for carbonaceous particles and polycyclic aromatic hydrocarbons from residential coal combustion in China. Environmental Science and Technology 39, 1861–1867.

Conde, F.J., Ayala, J.H., Afonso, A.M., Gonzalez, V., 2005. Emissions of polycyclic aromatic hydrocarbons from combustion of agricultural and sylvicultural debris. Atmospheric Environment 39, 6654–6663.

Cooper, D.A., 2001. Exhaust emissions from high speed passenger ferries. Atmospheric Environment 35, 4189–4200.

Cotham, W.E., Bidleman, T.F., 1995. Polycyclic aromatic hydrocarbons and polychlorinated biphenyls in air at an urban and a rural site near Lake Michigan. Environmental Science and Technology 29, 2782–2789.

Crimmins, B.S., Dickerson, R.R., Doddridge, B.G., Baker, J.E., 2004. Particulate polycyclic aromatic hydrocarbons in the Atlantic and Indian Ocean atmospheres during the Indian Ocean Experiment and Aerosols99: continental sources to the marine atmosphere. Journal of Geophysical Research 109, D05308.

Daisey, J.M., McCaffrey, R.J., Gallagher, R.A., 1981. Polycyclic aromatic hydrocarbons and total extractable particulate organic matter in the Arctic aerosol. Atmospheric Environment 15, 1353–1363.

Draxler, R. R., Rolph, G. D., 2003. HYSPLIT (HYbrid Single-Particle Lagrangian Integrated Trajectory) Model access via NOAA ARL READY Website (http://www.arl.noaa.gov/ready/hysplit4.html). NOAA Air Resources Laboratory, Silver Spring, MD.

Grimmer, G., Jacob, J., Naujack, K.W., Dettbarn, G., 1983. Determination of polycyclic aromatic compounds emitted from brown-coal-fired residential stoves by gas chromatography/mass spectrometry. Analytical Chemistry 55, 892–900.

Goldan, P.D., Parrish, D.D., Kuster, W.C., Trainer, M., McKeen, S.A., Holloway, J., Jobson, B.T., Sueper, D.T., Fehsenfeld, F.C., 2000. Airborne measurements of isoprene, CO, and anthropogenic hydrocarbons and their implications. Journal of Geophysical Research 105 (D7), 9091–9105.

Guo, Z.G., Sheng, L.F., Feng, J.L., Fang, M., 2003. Seasonal variation of solvent extractable organic compounds in the aerosols in Qingdao, China. Atmospheric Environment 37, 1825–1834.

Halsall, C.J., Coleman, P.J., Davis, B.J., Burnett, V., Waterhouse, K.S., Harding-Jones, P., Jones, K.C., 1994. Polycyclic aromatic hydrocarbons in U.K. urban air. Environmental Science and Technology 28, 2380–2386.

Halsall, C.J., Barrie, L.A., Fellin, P., Muir, D.C.G., Billeck, B.N., Lockhart, L., Rovinsky, F.Y., Kononov, E.Y., Pastukhov, B., 1997. Spatial and temporal variation of polycyclic aromatic hydrocarbons in the Arctic atmosphere. Environmental Science and Technology 31, 3593–3599.

Jaward, F.M., Barber, J.L., Booij, K., Jones, K.C., 2004. Spatial distribution of atmospheric PAHs and PCNs along a north–south Atlantic transect. Environmental Pollution 132, 173–181.

Kamens, R.M., Guo, Z., Fulcher, J.N., Bell, D.A., 1988. The influence of humidity, sunlight, and temperature on the daytime decay of polyaromatic hydrocarbons on atmospheric soot particles. Environmental Science and Technology 22, 103–108.

Khalili, N.R., Scheff, P.A., Holsen, T.M., 1995. PAH source fingerprints for coke ovens, diesel and, gasoline engines, highway tunnels, and wood combustion emissions. Atmospheric Environment 29, 533–542.

Laflamme, R.E., Hites, R.A., 1978. The global distribution of polycyclic aromatic hydrocarbons in recent sediments. Geochimica et Cosmochimica Acta 42, 289–303.

Lohmann, R., Northcott, G.L., Jones, K.C., 2000. Assessing the contribution of diffuse domestic burning as a source of PCDD/Fs, PCBs, and PAHs to the U.K. atmosphere. Environmental Science and Technology 34, 2892–2899.

Lohmann, R., Jaward, F.M., Durham, L., Barber, J.L., Ockenden, W., Jones, K.C., Bruhn, R., Lakaschus, S., Dachs, J., Booij, K., 2004. Potential contamination of shipboard air samples by diffusive emissions of PCBs and other organic pollutants: implications and solutions. Environmental Science and Technology 38, 3965–3970.

Mai, B.X., Qi, S.H., Zeng, E.Y., Yang, Q.S., Zhang, G., Fu, J.M., Sheng, G.Y., Peng, P.A., Wang, Z.S., 2003. Distribution of polycyclic aromatic hydrocarbons in the coastal region off Macao, China: assessment of input sources and transport pathways using compositional analysis. Environmental Science and Technology 37, 4855–4863.

Masclet, P., Mouvier, G., Nikolaou, K., 1986. Relative decay index and sources of polycyclic aromatic hydrocarbons. Atmospheric Environment 20, 439–446.

Motelay-Massei, A., Ollivon, D., Garban, B., Teil, M.J., Blanchard, M., Chevreuil, M., 2004. Distribution and spatial trends of PAHs and PCBs in soils in the Seine River basin, France. Chemosphere 55, 555–565.

Ohura, T., Amagai, T., Fusaya, M., Matsushita, H., 2004. Spatial distributions and profiles of atmospheric polycyclic aromatic hydrocarbons in two industrial cities in Japan. Environmental Science and Technology 38, 49–55.

Okona-Mensah, K.B., Battershill, J., Boobis, A., Fielder, R., 2005. An approach to investigating the importance of high potency polycyclic aromatic hydrocarbons (PAHs) in the induction of lung cancer by air pollution. Food and Chemical Toxicology 43, 1103–1116.

Oros, D.R., Simoneit, B.R.T., 2000. Identification and emission rates of molecular tracers in coal smoke particulate matter. Fuel 79, 515–536.

Page, D.S., Huggett, R.J., Stegeman, J.J., Parker, K.R., Woodin, B., Brown, J.S., Bence, A.E., 2004. Sources of polycyclic aromatic hydrocarbons related to biomarker levels in fish from Prince William Sound and the Gulf of Alaska. Marine Environmental Research 58, 313–314.

Park, S.S., Kim, Y.J., Kang, C.H., 2002. Atmospheric polycyclic aromatic hydrocarbons in Seoul, Korea. Atmospheric Environment 36, 2917–2924.

Perera, F., Tang, D.L., Whyatt, R., Lederman, S.A., Jedrychowski, W., 2005. DNA damage from polycyclic aromatic hydrocarbons measured by benzo[a]pyrene-DNA adducts in mothers and newborns from Northern manhattan, The World Trade Center area, Poland, and China. Cancer Epidemiology Biomarkers and Prevention 14, 709–714.

Schauer, J.J., Rogge, W.F., Hildemann, L.M., Mazurek, M.A., Cass, G.R., Simoneit, B.R.T., 1996. Source apportionment of airborne particulate matter using organic compounds as tracers. Atmospheric Environment 30, 3837–3855.

Simcik, M.F., Eisenreich, S.J., Lioy, P.J., 1999. Source apportionment and source/sink relationships of PAHs in the coastal atmosphere of Chicago and Lake Michigan. Atmospheric Environment 33, 5071–5079.

Simoneit, B.R.T., 1984. Organic matter of the troposphere—III Characterization and sources of petroleum and pyrogenic residues in aerosols over the western united states. Atmospheric Environment 18, 51–67.

Slater, J.F., Currie, L.A., Dibb, J.E., Benner, J.B.A., 2002. Distinguishing the relative contribution of fossil fuel and biomass combustion aerosols deposited at Summit, Greenland through isotopic and molecular characterization of insoluble carbon. Atmospheric Environment 36, 4463–4477.

Stohl, A., Eckhardt, S., Forster, C., James, P., Spichtinger, N., Seibert, P., 2002. A replacement for simple back trajectory calculations in the interpretation of atmospheric trace substance measurements. Atmospheric Environment 36, 4635–4648.

Wang, X., Ding, X., Mai, B., Xie, Z., Xiang, C., Sun, L., Sheng, G., Fu, J., Zeng, E.Y., 2005. Polybrominated diphenyl ethers in airborne particulates collected during a research expedition from Bohai Sea to the Arctic. Environmental Science and Technology 39, 7803–7809.

Wania, F., 2003. Assessing the potential of persistent organic chemicals for long-range transport and accumulation in polar regions. Environmental Science and Technology 37, 1344–1351.

Wania, F., Haugen, J.-E., Lei, Y.D., Mackay, D., 1998. Temperature dependence of atmospheric concentrations of semivolatile organic compounds. Environmental Science and Technology 32, 1013–1021.

Yunker, M.B., Macdonald, R.W., Vingarzan, R., Mitchell, R.H., Goyette, D., Sylvestre, S., 2002. PAHs in the Fraser River basin: a critical appraisal of PAH ratios as indicators of PAH source and composition. Organic Geochemistry 33, 489–515.